Biomass Conversion and Biorefinery (2023) 13:9765–9774
https://doi.org/10.1007/s13399-021-01833-y

ORIGINAL ARTICLE

Physicochemical characteristics of polysaccharides from catalytic and noncatalytic acetic acid-peroxide delignification of larch wood

Anna I. Chudina[1] · Yuriy N. Malyar[1,2] · Irina G. Sudakova[1] · Aleksandr S. Kazachenko[1,2] · Andrey M. Skripnikov[1,2] · Valentina S. Borovkova[1,2] · Alexander A. Kondrasenko[1] · Elena V. Mazurova[1] · Olga Yu. Fetisova[1] · Ivan P. Ivanov[1]

Received: 19 May 2021 / Revised: 26 July 2021 / Accepted: 28 July 2021 / Published online: 29 August 2021

Abstract

The composition and physicochemical characteristics of polysaccharides extracted from spent liquors of catalytic and noncatalytic delignification of larch wood in the acetic acid-hydrogen peroxide medium were studied. The following were used as catalysts: $(NH_4)_6Mo_7O_{24}$, $MnSO_4$, TiO_2, and $ZnSO_4$. The structure of polysaccharides was identified by FTIR and NMR spectroscopy. Their composition was established using gas chromatography, and the physicochemical characteristics were studied using gel permeation chromatography, scanning electron microscopy, thermogravimetric analysis, gas adsorption, and elemental analysis. It was shown that in the process of oxidative delignification, a significant amount of hemicelluloses and arabinogalactan passes into the spent liquor. The yield of polysaccharides was up to 16.9 wt%. Polysaccharides had a weight-average molecular weight of up to 22.9 kDa and a narrow molecular weight distribution.

Keywords Wood polysaccharides · Delignification · Hydrogen peroxide · Larch wood

1 Introduction

Hemicelluloses are polysaccharides in a plant cell wall that represent the most widespread, after cellulose, renewable plant polymers in the lignocellulosic materials. They are a type of heteropolysaccharides with a complex structure, which can contain glucose, xylose, mannose, galactose, arabinose, rhamnose, and glucuronic and galacturonic acids in different amounts, depending on a source. The dominant coniferous wood hemicelluloses are partially acetylated galactoglucomannans and glucomannans (up to 20−25% of the wood weight) [1] and arabinoglucuronoxylans (5−10% of the wood weight) [2]. Larch wood contains arabinogalactan in a fraction of 5−25% of the wood weight, depending on larch species [3].

The recent investigations showed the benefits of polymeric hemicelluloses and their potential for use in various fields. According to the data on the modification of hemicelluloses, these polymers can be used in production of new industrial materials, e.g., biomedical hydrogels [4] and biodegradable food wrap [5]. The unique colloidal properties of the galactoglucomannan extracted from spruce wood can be used in the development of functional nano- or microstructures separately or in combination with other components [6]. The spruce hemicelluloses have prospects for application such as partial substituents of synthetic polylactide in 3D printing [7] and for the treatment of chronic prostatic inflammation [8]. Deloule et al. [9] demonstrated the importance of softwood hemicelluloses as a potential source of prebiotics. Gautam et al. [10] used the hemicellulose extracted from pine needles as an effective adsorbent for removal of malachite green from wastewater. Mikkonen et al. [11] reported on new promising engineering emulsion systems for alkyd paints stabilized by the hemicelluloses extracted from birch and spruce.

In recent years, the extraction of hemicelluloses from wood raw materials has been studied intensively. Hemicelluloses were isolated by the hot-water extraction [12, 13], hot pressurized water pretreatment [14], alkaline hydrogen peroxide

---

✉ Yuriy N. Malyar
yumalyar@gmail.com

[1] Institute of Chemistry and Chemical Technology, Krasnoyarsk Science Center, Siberian Branch, Russian Academy of Sciences, Akademgorodok 50, bld. 24, Krasnoyarsk 660036, Russia

[2] Siberian Federal University, pr. Svobodny 79, Krasnoyarsk 660041, Russia

pretreatment [15], microwave-assisted extraction under atmospheric pressure [16, 17], and steam explosion extraction [18].

Currently, new methods of cellulose production are being developed, which is based on the peroxide delignification of wood in organic solvents, e.g., acetic and formic acids, and in the presence of various catalysts [19–21]. The treatment of wood with organic solvents as delignification media allows the lignocellulosic materials to be fractionated to produce lignin, cellulose, and hemicelluloses, thereby providing an excellent approach in terms of biomass use. The spent liquors consisting of soluble hemicelluloses and lignin depolymerization products do not contain toxic chlorine- and sulfur-containing compounds. Easy solvent recovery and environmental friendliness are important features of such processes [22].

A mixture of acetic acid and hydrogen peroxide is considered to be very effective in cleaving the aromatic rings of lignin and is also an environmentally friendly solvent [23]. Pretreatment with acetic acid with hydrogen peroxide is an effective approach to selectively remove lignin from biomass while retaining most of the carbohydrates [24, 25]. In addition, the presence of catalysts based on variable valence metals intensifies the delignification process due to the formation of peroxo complexes, which are strong oxidants and carry out the destruction of lignin [26, 27].

Studies [20, 21] were devoted to the oxidative catalytic delignification of various timber species in the hydrogen peroxide-acetic acid–water medium in the presence of the solid TiO_2 catalyst and the soluble $MnSO_4$ one. The study [19] compared the catalytic properties of the soluble ($CuSO_4$, $ZnSO_4$, $MnSO_4$, $FeSO_4$, and $(NH_4)_6Mo_7O_{24}$) and solid (TiO_2, KN-30, and C-FeZSM-5 zeolites) catalysts for delignification of wood including the same solvent. The main attention in these works was paid to the yield and composition of solid cellulosic products.

This study aimed to examine the composition, structure, and physicochemical characteristics of the polysaccharides extracted from the spent liquor of catalytic and noncatalytic acetic acid-peroxide delignification of larch wood.

2 Experimental

2.1 Raw materials

The raw material used was sawdust (a fraction of 2.0–5.0 mm) of the Siberian larch (Larix Sibirica) grown in the Krasnoyarsk Territory. The sawdust chemical composition was determined using conventional wood chemistry analytical methods [28]. The main larch wood components (wt%) were cellulose (41.2 ± 0.8), lignin (28.1 ± 0.6), polysaccharides, hydrolysable with 2% hydrochloric acid (26.4 ± 0.5), extractive substances (2.8 ± 0.0), and ash (0.8 ± 0.0).

A scheme of the oxidative catalytic fractionation of larch wood in the acetic acid-hydrogen peroxide medium with the formation of cellulose and polysaccharides is shown in Fig. 1.

2.2 Larch wood delignification

The shredded larch wood was delignified in a 250-mL glass reactor equipped with a stirrer and a reflux condenser. The delignification solution consisted of glacial acetic acid (30 wt%), hydrogen peroxide (6 wt%), and distilled water. The liquid wood ratio (LWR) was 15. In this study, we used four catalysts ($(NH_4)_6Mo_7O_{24}$, $MnSO_4$, TiO_2, and $ZnSO_4$), which demonstrate the high delignification efficiency, in a fraction of 1% of the wood weight. The delignification was performed for 4 h at temperatures of 90 °C and 100 °C under constant stirring. After completion of the delignification process, a solid residue (the cellulosic product) was separated from the spent liquor by filtration with a Buchner funnel, washing until neutral pH, and drying to the air-dry state.

2.3 Extraction of polysaccharides

The spent liquor (liquor 1 in Fig. 1) was concentrated on a rotary evaporator. Then, hot (about 60 °C) water was added at a volumetric ratio of 1:1 and driven off in a rotary evaporator. This procedure was performed twice to remove acetic acid. Polysaccharides were precipitated with a fivefold volume of ethanol (96% wt.) under slow stirring and then held for 12 h at a temperature of 4 °C. The obtained white curdled precipitate of polysaccharides was separated from the lignin depolymerization products (liquor 2 in Fig. 1) by filtration with a Buchner funnel, washed with ethanol, frozen, and dried in an Iney-6 freeze dryer. The yield of polysaccharides was determined in relation to the initial wood weight. The measurements were carried out in triplicate. Polysaccharides, obtained at a delignification temperature of 100 °C, were analyzed by Fourier-transform infrared (FTIR) and nuclear magnetic resonance (NMR) spectroscopy, gas chromatography (GC), gel permeation chromatography (GPC), scanning electron microscopy (SEM), and thermogravimetric analysis (TGA). The elemental composition and textural characteristics were examined.

2.4 Monosaccharide composition of polysaccharides

To determine the monosaccharide composition, the polysaccharides were hydrolyzed by the HCl solution (2%) for 3 h. The individual composition and monosaccharide content in the hydrolysates were determined on a VARIAN-450 GC gas chromatograph equipped with a flame ionization detector on a VF-624 ms capillary column with a length of 30 m and an inner diameter of 0.32 mm. A hydrolysate sample was

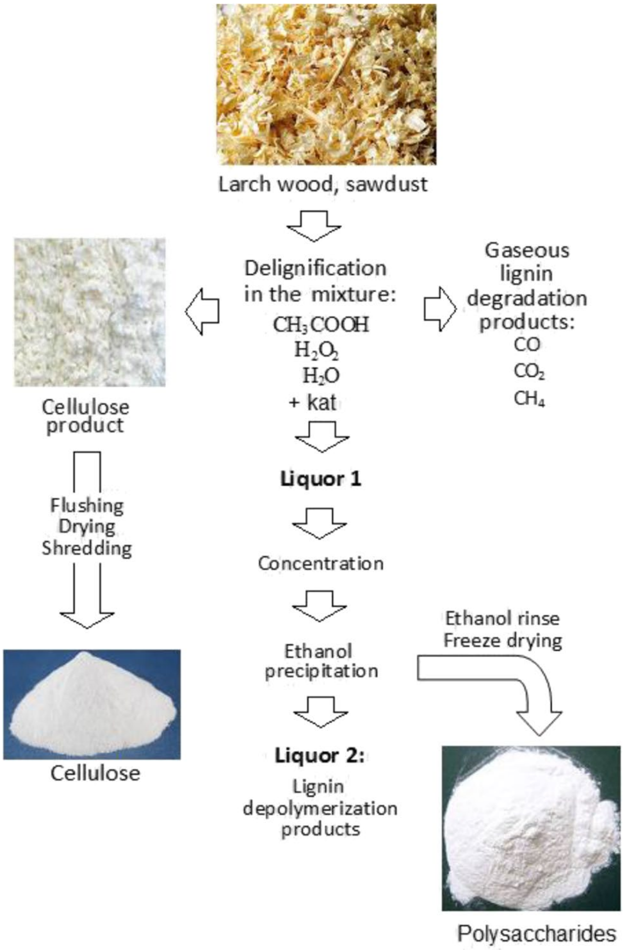

Fig. 1 Fractionation of larch wood in the acetic acid-hydrogen peroxide medium

pre-derivatized by the technique described in Ruiz-Matute et al. [29] with the formation of trimethylsilyl derivatives. The silylating reagent was a mixture of trimethylchlorosilane and hexamethyldisilazane in pyridine and sorbitol was used as an internal standard (IS). Standards for the analysis of the hydrolysates were glucose, arabinose, galactose, sorbitol, mannose, and xylose (Panreac, Germany).

2.5 Gel permeation chromatography

The weight-average molecular weight (M_w), number-average molecular weight (M_n), and polydispersity (PDI) of the polysaccharide samples were determined by GPC using an Agilent 1260 Infinity II Multi-Detector GPC/SEC System chromatograph with a refractive detector. The separation was made on two Agilent PL aquagel-OH columns using the solution of $0.2 M NaNO_3 + 0.01$ M NaH_2PO_4 in water (a pH of 7) as a mobile phase. The column was calibrated using the polyethylene glycol standards (Agilent, US). The eluent flow rate was 1 mL/min and the sample volume was 100 μL. Before the analysis, the samples were dissolved in the mobile phase (~ 5 mg/mL) and filtered through a 0.45-μm Agilent PES membrane filter (Millipore). The data collection and processing were performed using the Agilent GPC/SEC MDS software.

2.6 FTIR and NMR analysis of polysaccharides

The IR spectra were recorded on a Shimadzu IRTracer-100 FTIR spectrometer (Japan). Specimens for recording the IR absorption spectra were pressed in tablets containing 3 mg of the sample in a potassium bromide matrix. The NMR analysis (heteronuclear single quantum coherence (HSQC) spectroscopy) of polysaccharides was made on a Bruker Avance III 600 spectrometer (Germany). Before the analysis, the sample was completely dissolved in the DMSO-d6 solvent and placed into a 5-mm NMR tube at room temperature.

2.7 Elemental analysis

The elemental analysis of the polysaccharides isolated from the spent liquors of the catalytic and noncatalytic larch wood delignification was made on a Vario El Cube ELEMENTAR CHNSO analyzer (Germany).

2.8 Thermogravimetric analysis

The thermogravimetric analysis was made on a NETZSCH STA 449 F1 Jupiter simultaneous thermal analysis instrument (Germany). The polysaccharide samples were analyzed in argon at a heating rate of 10 °C · min^{-1}, temperatures from 30 to 900 °C, and protective and blowout gas flow rates of 20 and 50 mL • min^{-1}, respectively. The Al_2O_3 cylindrical crucible with a perforated cover was used and a reference was the empty corundum crucible with a cover. The instrument was calibrated according to the specification using reference substances supplied with the instrument. The mass of the samples for analysis was determined on a Sartorius BP121S analytical lab scale digital balance. The measurement results were processed using the NETZSCH. Proteus Thermal Analysis.5.1.0 software supplied with the instrument.

2.9 Analysis of the pore volume and surface area

The textural characteristics of polysaccharides were obtained using the nitrogen adsorption and desorption isotherms measured on a Micromeritics ASAP 2020 automatic adsorption analyzer (US) at 77 K under relative pressures of $P/P_0 = 5 \bullet 10^{-6}$—0.998. Before the adsorption measurements, the samples were degassed in vacuum for 12 h at 90 °C. The parameters used to identify the porous structure of the samples were specific surface area S_{BET} and average pore size D_{pore} [30]. The total pore volume V_{tot} calculated by a single-point technique from the volume of nitrogen adsorbed under a relative pressure of $P/P_0 \geq 0.98$. The micropore volume V_{micro} was calculated by the t-plot method [31].

2.10 Scanning electron microscopy

The morphology of the polysaccharide samples was identified on a Hitachi S5500 scanning electron microscope (Japan) with a cold tungsten cathode equipped with a Hitachi BF/DF DUO-STEM STEM detector at a variable electron collection angle, an accelerating voltage of 30 kV, and a spatial resolution of 0.4 nm in secondary-electron imaging.

3 Results and discussion

3.1 Delignification and yield of polysaccharides

The polysaccharides were extracted from the spent liquors of the catalytic and noncatalytic larch wood delignification after the cellulose isolation. The conditions for delignification were chosen on the basis of earlier study [19], where it was shown that, at a temperature of 100 °C, a hydrogen peroxide content of 6 wt%, an acetic acid of 30 wt%, and a LWR of 15, the deepest delignification of wood occurs, which ensures a residual lignin content below 1% in the cellulose product. In this case, water-soluble low-molecular-weight lignin degradation products, as well as polysaccharides, pass into the solution. The dissolved polysaccharides were isolated from the spent liquor by ethanol precipitation.

Table 1 Yields of polysaccharides from the spent liquors of larch wood delignification at process temperatures of 90 °C and 100 °C

Samples	Polysaccharides yield (wt%)[a]	
	90 °C	100 °C
PS_{nocat}[b]	12.6 ± 0.3	15.2 ± 0.5
PS_{Mo}[c]	15.6 ± 0.5	16.9 ± 0.5
PS_{Mn}[d]	15.2 ± 0.5	16.5 ± 0.5
PS_{Ti}[e]	13.4 ± 0.4	15.8 ± 0.5
PS_{Zn}[f]	13.9 ± 0.4	14.2 ± 0.4

[a] Relative to the initial air-dry larch wood

[b] The polysaccharides obtained by noncatalytic delignification

[c] The polysaccharides obtained in the presence of the $(NH_4)_6Mo_7O_{24}$ catalyst

[d] The polysaccharides obtained in the presence of the $MnSO_4$ catalyst

[e] The polysaccharides obtained in the presence of the TiO_2 catalyst

[f] The polysaccharides obtained in the presence of the $ZnSO_4$ catalyst

The yields of polysaccharides extracted from the spent liquors of the oxidative catalytic and noncatalytic larch wood delignification are given in Table 1.

As shown in Table 1, the polysaccharide yield at a process temperature of 90 °C is lower than that at 100 °C. This is due to the fact that at 100 °C the process of wood delignification is more complete [19, 20] and, therefore, a greater amount of structural polysaccharides passes into liquor 1. The use of the $(NH_4)_6Mo_7O_{24}$ and $MnSO_4$ catalysts ensures a fairly high yield of polysaccharides already at 90 °C. The TiO_2 catalyst works much more efficiently at 100 °C than at 90 °C. When the $ZnSO_4$ catalyst is used, the polysaccharide yield is at the lowest, which is apparently related to the strong destructive effect of this catalyst on polysaccharides.

3.2 Carbohydrate composition of polysaccharide mixture

The carbohydrate composition of the polysaccharides obtained by the oxidative catalytic and noncatalytic delignification of larch wood is illustrated in Fig. 2.

According to the literature data, the mannose:galactose:glucose ratio in galactoglucomannan of conifers is 3:1:1 and the galactose:arabinose ratio in arabinogalactan of larch wood is 6:1 [2, 3]. The high galactose and mannose contents in the samples show that galactoglucomannan and arabinogalactan are the predominant polysaccharides isolated from spent liquor. The presence of xylose is indicative of the presence of small amounts of arabinoglucuronoxylan, which is also a typical representative of softwood hemicelluloses. We see that the polysaccharides we have isolated are a mixture of structural wood polysaccharides (hemicelluloses) and arabinogalactan, which is an extractive polysaccharide. The lower galactose and arabinose contents in the polysaccharide mixture obtained with $ZnSO_4$ suggest that this catalyst apparently degrades arabinogalactan stronger.

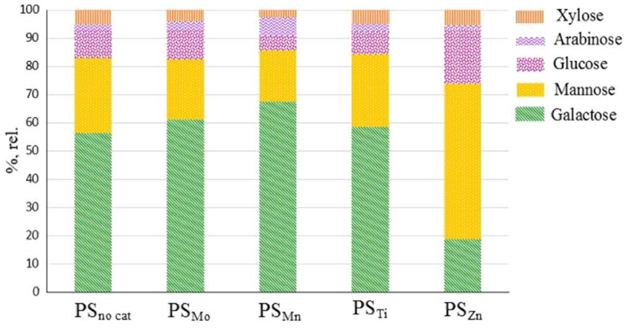

Fig. 2 Monosaccharide composition of the polysaccharides extracted from the spent liquor of the oxidative catalytic and noncatalytic delignification of larch wood (% relative to the total monosaccharide content)

3.3 FTIR and NMR spectroscopy of polysaccharides

The FTIR spectra of the samples contain all bands characteristic of heteropolysaccharides (Fig. 3), which are described in detail in [18, 32–35]. The absorption bands at 3433 and 2924 cm^{-1} refer to the O–H and C–H stretching, respectively. The bands at 1377 and 1245 cm^{-1} correspond to the O–H and C–O bending in polysaccharides. The band at 893 cm^{-1} corresponds to the vibrations of the C1 atom and four surrounding atoms, which is typical of the β-glycosidic bonds between sugar molecules. It can be seen that all the polysaccharide samples are acetylated, which is reflected in the three acetyl ether bands at 1736 cm^{-1} (ester $C=O$), 1377 cm^{-1} (–C–CH_3), and 1245 cm^{-1}(–C–O–, the stretching band). The band at 1635 cm^{-1} corresponds to the absorbed water bending. The band at 1075 cm^{-1} corresponds to stretching of the C–O bond in the HC–OH group of the pyranose ring. The polysaccharide samples are free of residual lignin since the spectra do not include the lignin absorption band at 1520 cm^{-1}.

The HSQC NMR study allowed us to identify and compare the polysaccharide structures (Fig. 4). The HSQC spectra contain typical light circles expected for polysaccharide fragments; the cross-peak signals were assigned according to reliable works [36–38]. The spectral region δC/δH 55–82/2.9–3.9 contains the signals characteristic of C2, C3, and C4 mannose, galactose, glucose, xylose, and arabinose atoms. The spectral region δC/δH 61–63/3.15–3.9 contains the signals from C5 and C6 carbohydrate atoms. The H1/C1 cross peaks assigned to the mannose, glucose, galactose, and xylose molecules were observed at 4.75/99.0, 4.55/101.0, 4.29/103.0, and 4.16/103.1 ppm, respectively.

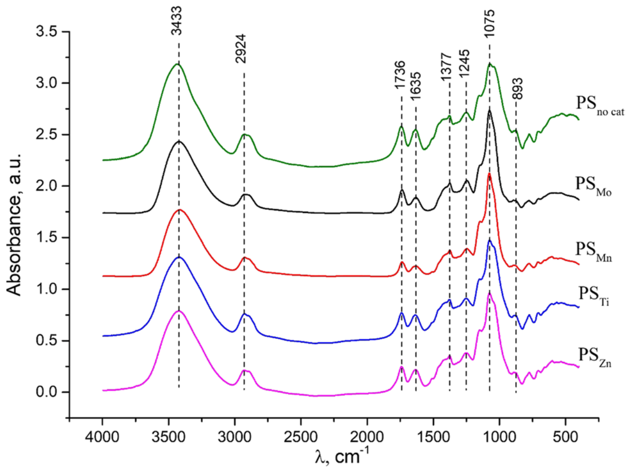

Fig. 3 FTIR spectra of the polysaccharides obtained by the oxidative catalytic and noncatalytic delignification of larch wood

The two peaks at δC/ δH 71.3/5.38 and 73.0/4.75 ppm in the spectra indicate that the hydroxyl groups on carbon 2 and 3 of mannose links are partially acetylated in all the samples. Such an acetylation type is typical of native hemicelluloses of coniferous wood. The spectrum of the sample obtained with the $MnSO_4$ catalyst includes no signals of carbon atoms associated with the acetyl groups and C1 carbohydrate atoms. This is apparently due to the fact that manganese forms complexes with polysaccharides, which leads to the paramagnetic broadening of the NMR signals and complicates their observation. Such complexes were described for arabinogalactan in Mercê et al. [39].

3.4 Molecular weight distribution

To illustrate the degree of depolymerization of the polysaccharides at the catalytic and noncatalytic delignification of larch wood, the molecular weights were determined by GPC using a refractive detector. The obtained weight- and number-average molecular weights of the polysaccharide samples and the polydispersity indices are given in Table 2.

According to the literature data, the weight-average molar weight M_w of native acetylated galactoglucomannan can lie between 20 and 50 kDa [1, 3] and for arabinogalactan, between 20 and 100 kDa [3]. Chadni et al. [16] studied the hemicelluloses isolated from spruce sawdust in a neutral medium at 100 °C for 1 h with presoaking and reported an M_n value of 20.730 kDa, an M_w value of 37.870 kDa, and a PDI of 1.82 for them. In the study [18], the same research team examined the effect of steam explosion conditions on the extraction of hemicelluloses from spruce sawdust,the weight-average molecular weight M_w of hemicelluloses obtained in a neutral medium was found to be 9–27 kDa and the PDI value was 2.3–2.6. The work [40] studied the high-temperature extraction of galactoglucomannan from pine wood. M_w at optimum extraction parameters of 7 kDa at 170° and an extraction time of 20 min.

Treatment with an organic acid in an oxidizing environment in the presence of various catalysts results in leads to partial destruction of the macromolecular structure of polysaccharides, which is associated with the rupture of glycosidic bonds between polysaccharide molecules. This is especially the case for the polysaccharides obtained with the soluble catalysts $(NH_4)_6Mo_7O_{24}$, $MnSO_4$, and $ZnSO_4$. The number-average molecular weights M_n of the obtained polysaccharides range from 11.985 to 14.150 kDa and the weight-average molecular weights M_w from 1.584 to 22.946 kDa. The low (1.31–1.65) polydispersity indices indicate that the isolated polysaccharides are uniform in the molecular weight. Molecular

Fig. 4 HSQC NMR spectra of the polysaccharides obtained by the oxidative catalytic and noncatalytic delignification of larch wood

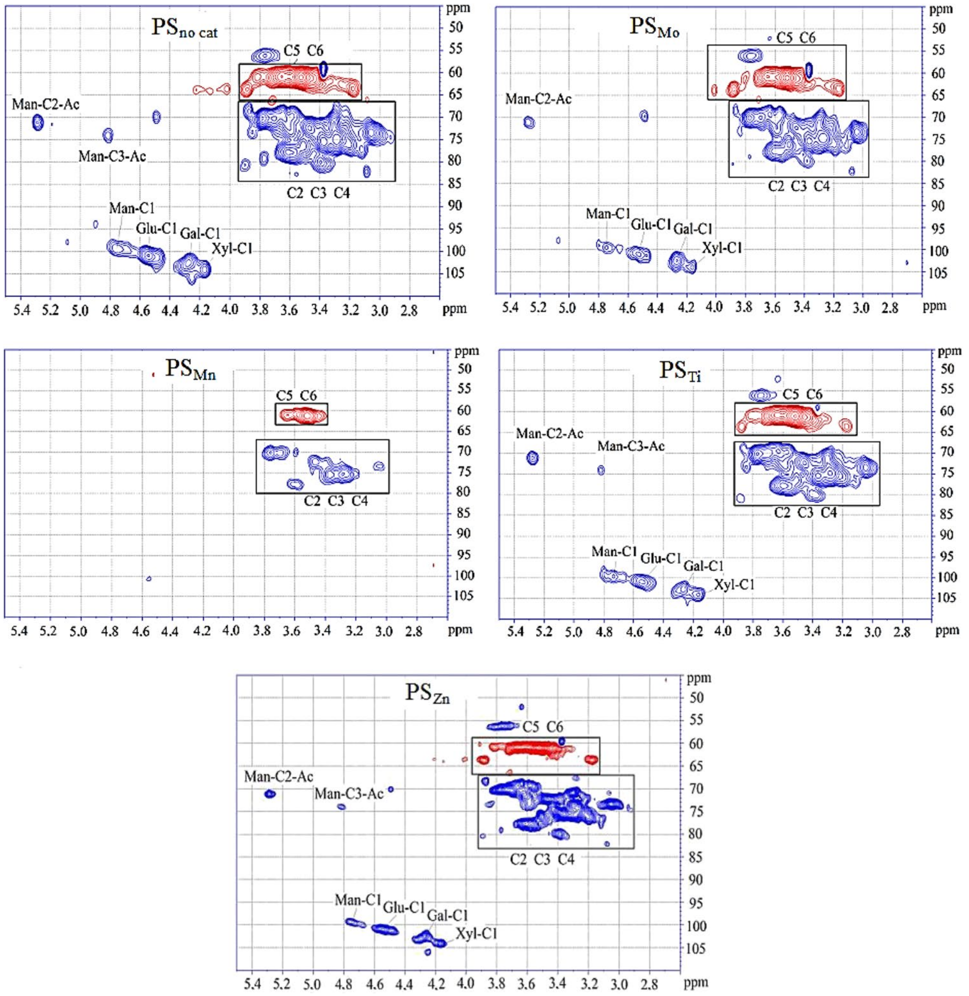

weight distribution curves of larch wood polysaccharides obtained by catalytic and noncatalytic delignification are shown in Fig. 5.

3.5 Elemental composition

The elemental composition of the polysaccharides isolated from the spent liquors of the catalytic and noncatalytic delignification of larch wood is given in Table 3. The polysaccharides isolated from the spent liquors of the noncatalytic delignification and in the presence of the

Table 2 Number-average (M_n) and weight-average (M_w) molecular weights and polydispersity indices (PDI) of the polysaccharide samples

Samples	M_n, kDa	M_w, kDa	PDI
$PS_{no\ cat}$	13.896	22.946	1.65
PS_{Mo}	11.985	16.584	1.38
PS_{Mn}	12.939	16.952	1.31
PS_{Ti}	14.150	18.846	1.33
PS_{Zn}	13.080	17.551	1.34

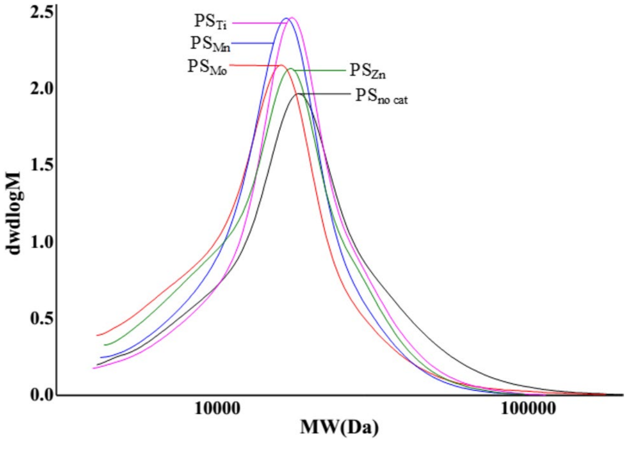

Fig. 5 Molecular weight distribution curves of the polysaccharides obtained by the oxidative catalytic and noncatalytic delignification of larch wood

Table 3 Carbon, hydrogen, and oxygen contents in the polysaccharide samples and H/C and O/C atomic ratios

Samples	C, %	H, %	O^a, %	H/C	O/C
PS$_{\text{no cat}}$	48.3	6.5	45.2	1.61	0.70
PS$_{\text{Mo}}$	55.7	6.0	38.3	1.28	0.52
PS$_{\text{Mn}}$	64.4	6.4	29.2	1.19	0.34
PS$_{\text{Ti}}$	42.2	6.4	51.4	1.83	0.91
PS$_{\text{Zn}}$	67.4	6.4	26.2	1.13	0.29

[a] Calculated from the difference, 100% −C,% −H,% −A^d(ash)

solid TiO$_2$ catalyst have the high H/C and O/C atomic ratios (Table 3). This points out that the destruction of the polysaccharide macromolecular structure occurs mainly via detaching the side chains with the acetylation of the end groups [41]. When the soluble (NH$_4$)$_6$Mo$_7$O$_{24}$, MnSO$_4$, and ZnSO$_4$ catalysts are used, the glycosidic bonds between the main polysaccharides chain links appear to be depolymerized, which is consistent with their lower molecular weights (Table 2).

3.6 Thermal analysis of polysaccharides

The thermal properties of the polysaccharide samples were studied by TGA. Figure 6 presents the derivative thermogravimetric (DTG) and thermogravimetric (TG) curves for the polysaccharides isolated from the spent liquors.

The polysaccharides extracted from larch wood are resistant to the heat up to ~ 200 °C and, upon further heating, begin destructing at an increasing rate. The thermal decomposition of the polysaccharide samples can be divided into three phases. In the first phase, the weight loss observed up to 100 °C is caused by evaporation of adsorbed water. In the second phase, the intense decomposition of the polysaccharides occurs, which begins at ~ 200 °C for all the samples. As the temperature increases above 200 °C, the thermal destruction reactions with hemolytic opening of the glycosidic and C−C bonds in the monosaccharide links already occur [42]. In the investigated polysaccharide samples, the most rapid weight loss was observed at 280−313 °C. The intense decomposition ends at a temperature of ~ 390 °C for the four samples and 420 °C for the sample obtained with ZnSO$_4$. In the last phase, when the temperature exceeds 390 °C, the weight loss is insignificant and the removal of volatiles occurs until the temperature reaches 899.8 °C. Table 4 gives the data of the main stages of decomposition of the polysaccharides extracted from the spent liquor of the catalytic and noncatalytic larch wood delignification.

The presented results show that polysaccharides obtained with TiO$_2$ and without catalyst have higher thermal stability. The lowest thermal stability is observed in the samples obtained with (NH$_4$)$_6$Mo$_7$O$_{24}$ and ZnSO$_4$.

3.7 Pore volume and surface area

Specific surface area S$_{\text{BET}}$, pore size distribution, and total pore volume are important indicators for further modification of polysaccharides and creation of composites.

The data given in Table 5 show that the textural characteristics of the polysaccharides extracted from the spent liquors of the catalytic and noncatalytic delignification of larch wood are very close. All samples contain a small amount of micropores. The lowest surface area is observed for the PS$_{\text{Zn}}$ sample, which is consistent with the analysis of the monosaccharide composition of this sample (see *3.2*). The analysis showed that the PS$_{\text{Zn}}$ sample contained less arabinogalactan, which is a more branched polysaccharide than galactoglucomannan.

3.8 Scanning electron microscopy

Polysaccharides extracted from spent liquors of oxidative catalytic and noncatalytic larch wood delignification were also studied by the SEM method. SEM images (Fig. S2)

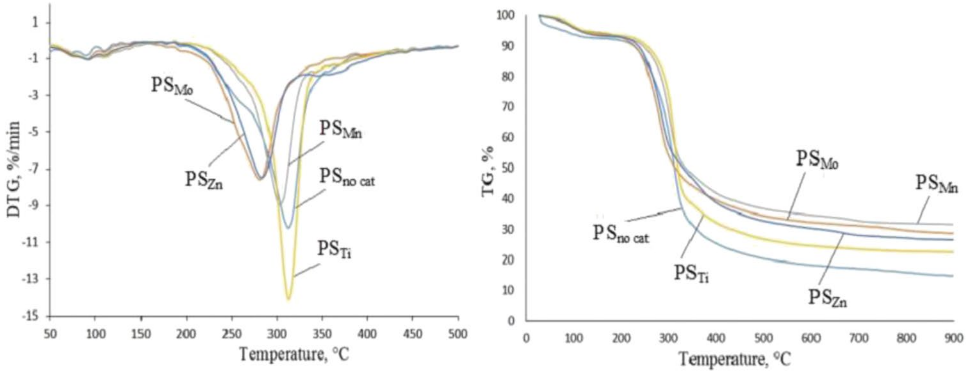

Fig. 6 DTG and TG curves of the polysaccharides extracted from the spent liquor of the catalytic and noncatalytic larch wood delignification

Table 4 TGA data on the polysaccharides obtained by catalytic and noncatalytic larch wood delignification

Samples	T_{beg}, °C	T_{end}, °C	T_{max}, °C	M_{M}, %	M_r
$PS_{no\ cat}$	200	389	313	45	14.7
PS_{Mo}	198	383	280	36	28.6
PS_{Mn}	202	390	302	34	31.6
PS_{Ti}	203	389	312	41	22.5
PS_{Zn}	198	420	282	31	26.5

T_{beg} is the temperature of the beginning of the intense weight loss, according to the DTG curve

T_{end} is the temperature of the end of the intense decomposition, according to the DTG curve

T_{max} is the temperature of the maximum rate of weight loss, according to the DTG curve

M_M is the weight loss at T_{max}, according to the TG curve

M_r is the residual sample mass at 899.8 °C (%)

show irregular coral formations that are hierarchical and indicate a highly branched amorphous polysaccharide structure.

The obtained polysaccharides can be used for the synthesis of sulfated derivatives that have anticoagulant properties and other types of biological activity [43]. Glucomannans can be candidates for use as potential therapeutic agents for the treatment of a number of physiological disorders [44], and they are widely used in the food industry [45]. It is also noted that heteropolysaccharides consisting of glucose, galactose, mannose, arabinose, rhamnose, xylose, and other monosaccharides have anticancer activity [46, 47].

4 Conclusions

Polysaccharides isolated from the spent liquors of catalytic and noncatalytic larch wood delignification are a mixture of structural polysaccharides and arabinogalactan. The polysaccharide yield ranges from 12.6 to 16.9 wt%, depending on the process temperature and the catalyst used. The catalyst used affects the molecular weight, elemental and monosaccharide composition, and textural and thermal properties of polysaccharides.

Table 5 Surface area, pore size, and pore volume of the polysaccharides

Samples	S_{BET}, m^2/g	V_{tot}, cm^3/g	V_{micro}, cm^3/g	D_{pore}, nm
$PS_{no\ cat}$	28.0	0.07	0.0009	5.1
PS_{Mo}	27.1	0.06	0.0010	4.5
PS_{Mn}	32.0	0.07	0.0015	4.6
PS_{Ti}	20.3	0.05	0.0006	5.0
PS_{Zn}	4.1	0.01	0.0004	5.1

PS_{Mn} has the highest content of galactose and arabinose and the lowest content of mannose; PS_{Zn} has the highest content of mannose and glucose and the lowest content of galactose. The structure of polysaccharides was identified by FTIR and NMR spectroscopy. FTIR spectroscopy showed the absence of absorption bands of phenylpropane units, which indicates that the polysaccharide samples do not contain residual lignin. DTG analysis shows that PS_{Ti} and $PS_{no\ cat}$ have higher thermal stability, while PS_{Mo} and PS_{Zn} show lower thermal stability. PS_{Ti} and $PS_{no\ cat}$ have a weight-average molecular weight M_w of 18.80 and 22.9 kDa and a polydispersity index of 1.33 and 1.65, respectively. PS_{Mo}, PS_{Mn}, and PS_{Zn} have lower molecular weights M_w 16.5–17.5 kDa and polydispersity index 1.31–1.38. The specific surface area S_{BET} for $PS_{no\ cat}$, PS_{Mo}, PS_{Mn}, and PS_{Ti} was 20.3–32.0 m^2/g, and for PS_{Zn} – 4.1 m^2/g, which is associated with the lowest content of arabinogalactan.

These polysaccharides can be used to create bioactive composites, multicomponent coatings, and fillers for the food and pharmaceutical industries.

Supplementary Information The online version contains supplementary material available at https://doi.org/10.1007/s13399-021-01833-y.

Acknowledgements FTIR and NMR analysis, gel permeation chromatography, elemental and thermogravimetric analysis, and SEM observations were done using the equipment of Krasnoyarsk Regional Research Equipment Centre of SB RAS.

Funding The reported study was funded by RFBR, project number 20–33-70256. This work was conducted within the framework of the budget project # 0287–2021-0012 for Institute of Chemistry and Chemical Technology SB RAS.

Declarations

Competing interests The authors declare no competing interests.

References

1. Willför S, Sundberg K, Tenkanen M, Holmbom B (2008) Spruce-derived mannans – a potential raw material for hydrocolloids and novel advanced natural materials. Carbohyd Polym 72:197–210
2. Bajpai P (2018) Chapter 2 - Wood and fiber fundamentals. In: Bajpai P (ed) Biermann's handbook of pulp and paper, 3rd edn. Elsevier, pp 19–74
3. Timell TE (1967) Recent progress in the chemistry of wood hemicelluloses. Wood Sci Technol 1:45–70
4. Markstedt K, Xu W, Liu J, Xu C, Gatenholm P (2017) Synthesis of tunable hydrogels based on O-acetyl-galactoglucomannans from spruce. Carbohyd Polym 157:1349–1357
5. Mendes FRS, Bastos MSR, Mendes LG, Silva ARA, Sousa FD, Monteiro-Moreira ACO, Cheng HN, Biswas A, Moreira RA

(2017) Preparation and evaluation of hemicellulose films and their blends. Food Hydrocolloids 70:181–190

6. Bhattarai M, Valoppi F, Hirvonen S-P, Hietala S, Kilpeläinen P, Aseyev V, Mikkonen KS (2020) Time-dependent self-association of spruce galactoglucomannans depends on pH and mechanical shearing. Food Hydrocolloids 102:105607
7. Xu W, Pranovich A, Uppstu P, Wang X, Kronlund D, Hemming J, Öblom H, Moritz N, Preis M, Sandler N, Willför S, Xu C (2018) Novel biorenewable composite of wood polysaccharide and polylactic acid for three dimensional printing. Carbohyd Polym 187:51–58
8. Konkol Y, Vuorikoski H, Tuomela J, Holmbom B, Bernoulli J (2017) Galactoglucomannan-rich hemicellulose extract from Norway spruce (Picea abies) exerts beneficial effects on chronic prostatic inflammation and lower urinary tract symptoms in vivo. Int J Biol Macromol 101:222–229
9. Deloule V, Boisset C, Hannani D, Suau A, Le Gouellec A, Chroboczek J, Botté C, Yamaryo-Botté Y, Chirat C, Toussaint B (2020) Prebiotic role of softwood hemicellulose in healthy mice model. J Funct Foods 64:103688
10. Gautam D, Kumari S, Ram B, Chauhan GS, Chauhan K (2018) A new hemicellulose-based adsorbent for malachite green. J Environ Chem Eng 6:3889–3897
11. Mikkonen KS, Kirjoranta S, Xu C, Hemming J, Pranovich A, Bhattarai M, Peltonen L, Kilpeläinen P, Maina N, Tenkanen M, Lehtonen M, Willför S (2019) Environmentally-compatible alkyd paints stabilized by wood hemicelluloses. Ind Crops Prod 133:212–220
12. Krogell J, Korotkova E, Eränen K, Pranovich A, Salmi T, Murzin D, Willför S (2013) Intensification of hemicellulose hot-water extraction from spruce wood in a batch extractor – effects of wood particle size. Biores Technol 143:212–220
13. Song T, Pranovich A, Holmbom B (2011) Effects of pH control with phthalate buffers on hot-water extraction of hemicelluloses from spruce wood. Biores Technol 102:10518–10523
14. Gallina G, Cabeza Á, Grénman H, Biasi P, García-Serna J, Salmi T (2018) Hemicellulose extraction by hot pressurized water pretreatment at 160℃ for 10 different woods: yield and molecular weight. J Supercrit Fluids 133:716–725
15. Alvarez-Vasco C, Zhang X (2017) Alkaline hydrogen peroxide (AHP) pretreatment of softwood: enhanced enzymatic hydrolysability at low peroxide loadings. Biomass Bioenerg 96:96–102
16. Chadni M, Bals O, Ziegler-Devin I, Brosse N, Grimi N (2019a) Microwave-assisted extraction of high-molecular-weight hemicelluloses from spruce wood. C R Chim 22:574–584
17. Gulbrandsen TA, Johnsen IA, Opedal M, Toven K, Øyaas K, Pranovich A, Mikkola JP, Hoff B (2015) Extracting hemicelluloses from softwood and bagasse as oligosaccharides using pure water and microwave heating. Cellul Chem Technol 49:117–126
18. Chadni M, Grimi N, Bals O, Ziegler-Devin I, Brosse N (2019b) Steam explosion process for the selective extraction of hemicelluloses polymers from spruce sawdust. Ind Crops Prod 141:111–757
19. Kuznetsov BN, Sudakova IG, Garyntseva NV, Tarabanko VE, Yatsenkova OV, Djakovitch L, Rataboul F (2021) Processes of catalytic oxidation for the production of chemicals from softwood biomass. Catal Today 375:132–144. https://doi.org/10.1016/j.cattod.2020.05.044
20. Sudakova IG, Garyntseva NV, Chudina AI, Kuznetsov BN (2020) Experimental and mathematical optimization of the peroxide delignification of larch wood in the presence of $MnSO_4$ catalyst. Catal Ind 12:265–272
21. Kuznetsov BN, Sudakova IG, Yatsenkova OV, Garyntseva NV, Rataboul F, Djakovitch L (2018) Optimizing single-stage processes of microcrystalline cellulose production via the peroxide delignification of wood in the presence of a Titania Catalyst. Catal Ind 10:360–367
22. Vila C, Santos V, Parajó JC (2003) Simulation of an organosolv pulping process: generalized material balances and design calculations. Ind Eng Chem Res 42:349–356
23. Khama L, Bigot YL, Delmas M, Avignon G (2005) Delignification of wheat straw using a mixture of carboxylic acid and peroxoacids. Ind Crops Prod 21:9–15
24. Bragatto J, Segato F, Squina FM (2013) Production of xylooligosaccharides (XOS) from delignified sugarcane bagasse by peroxide-HAc process using recombinatant xylanase from *Bacillus subtilis*. Ind Crop Prod 51:123–129
25. Wen P, Zhang T, Wang J, Lian Z, Zhang J (2019) Production of xylooligosaccharides and monosaccharides from poplar by a two-step acetic acid and peroxide/acetic acid pretreatment. Biotechnol Biofuels 12:87
26. Suchy M, Argyropoulos DS (2002) Catalysis and activation of oxygen and peroxide delignification of chemical pulps: a review. Tappi J 1:16
27. Ma R, Xu Y, Zhang X (2015) Catalytic oxidation of biorefinery lignin to value-added chemicals to support sustainable biofuel production. Chemsuschem 8:24–51
28. Sjöström E, Alén R (1999) Analytical methods of wood chemistry, pulping, and papermaking. Springer, Berlin, Heidelberg
29. Ruiz-Matute AI, Hernández-Hernández O, Rodríguez-Sánchez S, Sanz ML, Martínez-Castro I (2011) Derivatization of carbohydrates for GC and GC–MS analyses. J Chromatogr B 879:1226–1240
30. Rouquerol J, Avnir D, Fairbridge CW, Everett DH, Haynes JH, Pernicone N, Ramsay JDF, Sing KSW, Unger KK (1994) Recommendations for the characterization of porous solids [IUPAC Recommendations 1994]. Pure Appl Chem 66:1739–1758. https://doi.org/10.1351/pac199466081739
31. Scherdel C, Reichenauer G, Wiener M (2010) Relationship between pore volumes and surface areas derived from the evaluation of N_2-sorption data by DR-, BET- and t-plot. Microporous Mesoporous Mater 132:572–575
32. Kačuráková M, Capek P, Sasinková V, Wellner N, Ebringerová A (2000) FT-IR study of plant cell wall model compounds: pectic polysaccharides and hemicelluloses. Carbohyd Polym 43:195–203
33. Muthu S, Renuga S (2014) Vibrational spectra and normal coordinate analysis of 2-hydroxy-3-(2-methoxyphenoxy) propyl carbamate. Spectrochim Acta Part A Mol Biomol Spectrosc 132:313–325
34. Oinonen P, Krawczyk H, Ek M, Henriksson G, Moriana R (2016) Bioinspired composites from cross-linked galactoglucomannan and microfibrillated cellulose: thermal, mechanical and oxygen barrier properties. Carbohyd Polym 136:146–153
35. Peng F, Ren J-L, Xu F, Bian J, Peng P, Sun R-C (2009) Comparative study of hemicelluloses obtained by graded ethanol precipitation from sugarcane bagasse. J Agric Food Chem 57:6305–6317
36. Capek P, Alföldi J, Lišková D (2002) An acetylated galactoglucomannan from Picea abies L. Karst. Carbohydr Res 337:1033–1037
37. Giummarella N, Lawoko M (2017) Structural insights on recalcitrance during hydrothermal hemicellulose extraction from wood. ACS Sustain Chem Eng 5:5156–5165
38. Tang S, Jiang M, Huang C, Lai C, Fan Y, Yong Q (2018) Characterization of arabinogalactans from Larix principis-rupprechtii and their effects on NO production by macrophages. Carbohyd Polym 200:408–415
39. Mercê ALR, Landaluze JS, Mangrich AS, Szpoganicz B, Sierakowski MR (2001) Complexes of arabinogalactan of Pereskia aculeata and Co^{2+}, Cu^{2+}, Mn^{2+}, and Ni^{2+}. Biores Technol 76:29–37
40. Benouadah N, Pranovich A, Aliouche D, Labidi J, Willför S (2021) Optimization of the extraction of galactoglucomannans from Pinus halepensis. Holzforschung 75:563–573

41. Xu F, Liu CF, Geng ZC, Sun JX, Sun RC, Hei BH, Lin L, Wu SB, Je J (2006) Characterisation of degraded organosolv hemicelluloses from wheat straw. Polym Degrad Stab 91:1880–1886
42. Yang H, Yan R, Chen H, Lee DH, Zheng C (2007) Characteristics of hemicellulose, cellulose and lignin pyrolysis. Fuel 86:1781–1788
43. Kazachenko AS, Malyar YN, Vasilyeva NY, Fetisova OY, Chudina AI, Sudakova IG, Antonov AV, Borovkova VS, Kuznetsova SA (2021) Isolation and sulfation of galactoglucomannan from larch wood (Larix sibirica). Wood Sci Technol 55:1091–1107
44. Tester RF, Al-Ghazzewi FH (2013) Mannans and health, with a special focus on glucomannans. Food Res Int 50:384–391
45. Singh S, Singh G, Arya SK (2018) Mannans: an overview of properties and application in food products. Int J Biol Macromol 119:79–95
46. Carlotto J, de Almeida Veiga A, de Souza LM, Cipriani TR (2020) Polysaccharide fractions from Handroanthus heptaphyllus and Handroanthus albus barks: structural characterization and cytotoxic activity. Int J Biol Macromol 165:849–856
47. Li N, Wang C, Georgiev MI, Bajpai VK, Tundis R, Simal-Gandara J, Lu X, Xiao J, Tang X, Qiao X (2021) Advances in dietary polysaccharides as anticancer agents: structure-activity relationship. Trends Food Sci Technol 111:360–377